34th Annual International Conference of the IEEE EMBS
San Diego, California USA, 28 August - 1 September, 2012

# Variational Level Set approach for Automatic Correction of Multiplicative and Additive Intensity Inhomogeneities in Brain MR Images

Nishant Verma, Matthew C. Cowperthwaite, Mia K. Markey, *Senior Member, IEEE*

*Abstract*— **Retrospective correction of intensity inhomogeneities in magnetic resonance images of the brain is an essential pre-processing step before any sophisticated image analysis task can be performed. A popular choice when defining the degradation model in MR images is to use multiplicative intensity inhomogeneities that slowly varying across the image domain; this approach has been extensively used for bias field estimation. However, such a multiplicative model is often insufficient given that some of the most dominant physical causes of intensity inhomogeneities in MRI (such as non-uniform excitation strength) have a non-linear relationship with the receptor signal intensity. In this study, we consider a linear image degradation model with multiplicative and additive intensity inhomogeneity components. We propose a variational level sets approach that combines estimation of intensity inhomogeneity components during the image segmentation process. The evaluation of proposed approach on real MR image datasets demonstrate accurate estimation of multiplicative and additive intensity inhomogeneities improving brain tissue segmentation.**

## I. INTRODUCTION

Magnetic Resonance Imaging (MRI) is the most commonly used neuro-imaging method for producing high contrast volumetric images of the brain. However, it is a difficult and highly time intensive process to extract important information from the large number of voxels in a typical MR data set. Automatic image analysis tools, whose goals are to extract clinically relevant information and better present it to physicians for diagnosis and treatment planning purposes have recently received significant attention as a promising avenue to overcome some of the limitations of manual inspection of MR images. However, pre-processing of MR images is typically required to minimize image artifacts (such as image noise, intensity inhomogeneities, partial volume effects, etc.), which often adversely affect the performance of image analysis tools.

Intensity inhomogeneities in MR images are one such adverse phenomena that manifest as smooth, relatively slowly changing intensity variations across the image domain. They are also commonly referred to as radio frequency (RF) inhomogeneity, intensity non-uniformity, bias field, and shading artifacts. The root causes of intensity inhomogeneities in MR images are due to non-uniform RF excitation, non-uniform coil receptor sensitivity, and standing wave effects [1], [2]. Other minor factors that can produce intensity inhomogeneities are eddy currents due to rapid switching of magnetic field gradients, patient induced electromagnetic interactions, and geometric distortions. Although these intensity variations have little effect on visual interpretation of MR images, they significantly degrade the performance of automated image analysis routines such as for segmentation or registration. Therefore, correction for intensity inhomogeneities is a necessary preprocessing step before conducting any sophisticated automatic image analyses.

The correction methods for intensity inhomogeneities can be broadly classified into prospective and retrospective methods. Prospective correction usually requires special imaging sequences using physical phantoms and multiple reception coils, with subsequent MRI scanner calibration after assessing the excitation field strength, and the non-uniformity of each reception coil [1], [2], [3]. Prospective methods can correct for static intensity variations occurring due to imperfections in the instrument, however they cannot deal with patient-induced intensity inhomogeneities and are often impractical in the clinical setting because they typically require considerably longer scanning routines. Retrospective correction methods, on the other hand, only use the information contained within the captured image and therefore can be used to correct any MR image. Retrospective correction methods are thus much more relevant for clinical use, however they have limited ability to distinguish between scanner and patient-induced inhomogeneities.

A variety of retrospective correction methods have been proposed in the literature. Homographic filtering methods have been proposed that assume the frequency spectrum of the bias field is different from that of the anatomical structures, which is often not true in MR images [4], [5], [6]. Polynomial spline fitting and hypersurface models have also been considered to model the bias field using a combination of manually and automatically selected reference points [6], [7]; histogram matching to minimize the squared residual error within a window of pixel intensities has also been considered as a solution to bias field correction [8]. A common approach is to estimate the intensity inhomogeneities during the process of image segmentation, and several maximum-likelihood (ML) and maximum *a posteriori* probability (MAP) approaches have been proposed that fit parametric

N. Verma is jointly affiliated with Dept. of Biomedical Engineering, The University of Texas at Austin and NeuroTexas Institute, St. David's HealthCare, Austin, Phone: 512-471-1711, vnishant@utexas.edu

M. K. Markey is with Dept. of Biomedical Engineering, The University of Texas at Austin, TX 78712, USA, Phone: 512-471-1711 mia.markey@utexas.edu

M. C. Cowperthwaite is with NeuroTexas Institute, St. David's HealthCare, Austin, TX 78705, USA. Matthew.Cowperthwaite@stdavids.com

978-1-4577-1787-1/12/$26.00 ©2012 IEEE

models to image regions and estimate model parameters via Expectation-Maximization (EM) algorithm [6], [7]. For a detailed discussion and comparison of existing methods, see [9].

Models of image formation typically consider a multiplicative bias field corrupting the image in combination with an additive noise component. The additive noise is often removed using frequency filtering, regularizations, and smooth model fitting [9]. Additionally, logarithmic transformations are often used to convert multiplicative terms into additive terms. However, the use of a multiplicative model may not be sufficient to correct for intensity inhomogeneities produced by a wide range of possible physical sources.

Generally, a linear relationship is assumed to exist between sensitivity of the reception coil and the measured signal intensity and, therefore, spatial variations in the coil sensitivity can be modeled using a multiplicative field that scales the measured signal intensity. However, intensity inhomogeneities introduced by RF non-uniformities cannot be exactly modeled using a multiplicative field because of the non-linear relationship between excitation field strength and measure signal intensity. The broad use of higher magnetic field strengths in MR imaging, increases the contributions in intensity inhomogeneties resulting from sources such as eddy currents, patient induced electromagnetic interactions, and geometric distortions which cant be estimated using multiplicative models in MR images.

In this study, we consider a linear image degradation model that uses a multiplicative and an additive component to model intensity inhomogeneity in the MR images. We propose a variational approach in a level set framework that combines the two tasks of intensity inhomogeneity correction and brain tissue segmentation.

## II. DESCRIPTION OF THE MODEL

### A. Problem Formulation

Let $I(x,y)$ be the actual MR image and $\tilde{I}(x,y)$ be the idealized uncorrupted image of the same object, related to each other by

$$I(x,y) = f(\tilde{I}(x,y)), \qquad (x,y) \in \Omega$$

where, $f(.)$ is the model of image degradation resulting from noise and artifacts, and $\Omega$ denotes the image domain. The goal of retrospective bias field correction is estimation of degradation function the $f(.)$, which can be used to recover the ideal image $\tilde{I}(x,y)$ using, $\tilde{I}(x,y) = f^{-1}(I(x,y))$. In prospective correction, the degradation model is experimentally estimated before capturing the image of interest, whereas in retrospective bias field correction the exact form of the degradation model is unknown a priori. In this study, we consider a linear degradation model consisting of additive and multiplicative intensity inhomogeneities and additive Gaussian noise,

$$I(x,y) = w_1(x,y)\tilde{I}(x,y) + w_2(x,y) + \eta(x,y) \qquad (1)$$

where, $w_1(x,y)$ and $w_2(x,y)$ are the multiplicative and additive components of intensity inhomogeneities, respectively, and $\eta(x,y)$ is Gaussian additive noise with zero mean $\int_\Omega \eta(x,y)dxdy = 0$. To account for tissue heterogeneities and partial volume effects in brain MR images, we represent $\tilde{I}(x,y)$ as distinct regions $R_j$ each with normally distributed intensities with means and covariances as $\vec{\Lambda}_j = \{c_j, \sigma_j\}$, $j = 1...n$. The terms in (1) can be estimated by minimizing an objective function that contains contributions from fitting and smoothness terms,

$$F_{energy} = F_{fit} + F_{smooth} \qquad (2)$$

where, $F_{fit}$ is equivalent to maximizing the joint log-likelihood over all image pixels,

$$F_{fit} = \sum_{j=1}^{n} \int_{(x,y)\in R_j} \big[log(\sigma_j) + \frac{(\tilde{I}(x,y) - c_j)^2}{2\sigma_j^2}\big] dxdy \qquad (3)$$

$F_{smooth}$ is the smoothness term that controls for the slowly varying intensity inhomogeneities,

$$\begin{aligned} F_{smooth} = v_1 \int_\Omega |\nabla w_1|^2 dxdy + v_2 \int_\Omega |D^2 w_1|^2 dxdy \\ + v_3 \int_\Omega |\nabla w_2|^2 dxdy + v_4 \int_\Omega |D^2 w_2|^2 dxdy \end{aligned} \qquad (4)$$

where, $D^2(.)$ is the Hessian operator defined as $D^2 w = \begin{pmatrix} w_{xx} & w_{xy} \\ w_{yx} & w_{yy} \end{pmatrix}$, and $|D^2 w| = \sqrt{w_{xx}^2 + 2w_{xy}^2 + w_{yy}^2}$.

### B. Active Contour Model and Level Set Formulation

We minimize the objective function (2) in an active contour framework to obtain the desired tissue segmentation and estimate the degradation model. In an active contour model, a curve $C$ evolves on the image domain $\Omega$ under an external force partitioning the image into two distinct regions: $C_{in}$ denoting the image region bounded by $C$, and $C_{out}$ denoting the image region outside of $C$. In the proposed active contour model, we minimize the following energy functional,

$$E(C) = \mu.Length(C) + \beta.Area(C_{in}) + F_{energy} \qquad (5)$$

where, $\mu, \beta \geq 0$ are fixed parameters. The first two terms are regularization terms that enforce local constraints on the curve, while $F_{energy}$ represents the external force on the curve. The minimization of the energy functional (5) is difficult in terms of the image regions $R_j$, $j = 1,..n$. Using a level set formulation [10] enables representation of the image regions $R_j$ and evolving curve $C$ in terms of a higher dimensional Lipschitz function $\Phi : \Omega \to R$ [6] such that

$$\Phi(x,y) = \begin{cases} = 0 & \text{at } C \\ > 0 & \text{inside } C, \\ < 0 & \text{outside } C \end{cases} \qquad (x,y) \in \Omega$$

The energy minimization can be solved using well-established variational methods [11]. In this study, we consider a two-phase problem with image regions $R_1$ and $R_2$

defined by $C_{in}$ and $C_{out}$, respectively. Using the Heaviside function $H$ and Dirac measure $\delta$:

$$H(z) = \begin{cases} 1 & \text{if z} > 0 \\ 0 & \text{if z} < 0 \end{cases}, \qquad \delta(z) = \frac{d}{dz}H(z)$$

we can represent the energy functional (5) in terms of $\Phi(x,y), H(x,y)$ and $\delta(x,y)$,

$$\begin{aligned} E(\Phi, w_1, w_2, \vec{\Lambda}_1, \vec{\Lambda}_2) &= \mu \int_\Omega \delta(\Phi)|\nabla\Phi| dxdy \\ &+ \beta \int_\Omega H(\Phi) dxdy + \lambda_1 \int_\Omega \frac{(I - w_2 - c_1 w_1)^2}{2w_1^2\sigma_1^2} H(\Phi) dxdy \\ &+ \lambda_2 \int_\Omega \frac{(I - w_2 - c_2 w_1)^2}{2w_1^2\sigma_2^2} H(-\Phi) dxdy \\ &+ \lambda_1 \int_\Omega log(\sigma_1) H(\Phi) dxdy + \lambda_2 \int_\Omega log(\sigma_2) H(-\Phi) dxdy \\ &+ v_1 \int_\Omega |\nabla w_1|^2 dxdy + v_2 \int_\Omega |D^2 w_1|^2 dxdy \\ &+ v_3 \int_\Omega |\nabla w_2|^2 dxdy + v_4 \int_\Omega |D^2 w_2|^2 dxdy \end{aligned} \tag{6}$$

The intensity distribution parameters $\Lambda_1$ and $\Lambda_2$ can be obtained by minimizing $E(\Phi, w_1, w_2, \vec{\Lambda}_1, \vec{\Lambda}_2)$ with respect to $c_j$ and $\sigma_j$, keeping $\Phi(x,y)$, $w_1(x,y)$ and $w_2(x,y)$ fixed.

$$\begin{aligned} c_1 &= \frac{\int_\Omega (I - w_2) H(\Phi) dxdy}{\int_\Omega w_1 H(\Phi) dxdy}, c_2 = \frac{\int_\Omega (I - w_2) H(-\Phi) dxdy}{\int_\Omega w_1 H(-\Phi) dxdy} \\ \sigma_1^2 &= \frac{\int_\Omega (I - w_2 - c_1 w_1)^2 H(\Phi) dxdy}{\int_\Omega w_1^2 H(\Phi) dxdy} \\ \sigma_2^2 &= \frac{\int_\Omega (I - w_2 - c_2 w_1)^2 H(-\Phi) dxdy}{\int_\Omega w_1^2 H(-\Phi) dxdy} \end{aligned} \tag{7}$$

Minimizing the energy functional (6) with respect to $\Phi$, $w_1$, and $w_2$ while keeping $\Lambda_1, \Lambda_2$ fixed, gives the associated Euler-Lagrange equations. Parameterization by an artificial time $t \geq 0$ gives the following update equations for $\Phi(x,y,t), w_1(x,y,t)$, and $w_2(x,y,t)$ in the gradient descent directions,

$$\begin{aligned} \frac{\partial w_1}{\partial t} &= \lambda_1 \frac{(I - w_2 - w_1 c_1)(I - w_2)}{w_1^3 \sigma_1^2} H(\Phi) + 2v_1 \Delta w_1 \\ &+ \lambda_2 \frac{(I - w_2 - w_1 c_2)(I - w_2)}{w_1^3 \sigma_2^2} H(-\Phi) - 2v_2 \Delta^2 w_1 \end{aligned} \tag{8}$$

$$\begin{aligned} \frac{\partial w_2}{\partial t} &= \lambda_1 \frac{(I - w_2 - w_1 c_1)}{w_1^2 \sigma_1^2} H(\Phi) + 2v_3 \Delta w_2 - 2v_4 \Delta^2 w_2 \\ &+ \lambda_2 \frac{(I - w_2 - w_1 c_2)}{w_1^2 \sigma_2^2} H(-\Phi) \end{aligned} \tag{9}$$

$$\begin{aligned} \frac{\partial \Phi}{\partial t} &= \delta(\Phi) \Big[ \mu \cdot div\Big(\frac{\nabla\Phi}{|\nabla\Phi|}\Big) - \beta + \lambda_2 log(\sigma_2) - \lambda_1 log(\sigma_1) \\ &- \lambda_1 \frac{(I - w_2 - w_1 c_1)^2}{2w_1^2\sigma_1^2} + \lambda_2 \frac{(I - w_2 - w_1 c_2)^2}{2w_1^2\sigma_2^2} \Big] \end{aligned} \tag{10}$$

where, $\Delta(.)$ denotes the Laplacian operator. We impose zero boundary conditions for the $1^{st}$, $2^{nd}$, and $3^{rd}$ order partial derivatives of $w_1$ and $w_2$ on $\partial\Omega$ to ensure smoothness on the boundaries. At $t = 0$, the initial level set, the multiplicative and the additive inhomogeneities are defined by $\Phi^0(x,y), w_1^0(x,y)$, and $w_2^0(x,y)$, respectively.

### C. Numerical Implementation

We use $C^\infty(\bar{\Omega})$ regularized versions of the Heaviside function and Dirac measure denoted by $H_\epsilon$ and $\delta_\epsilon$, as described in [12] for computing the associated Euler-Lagrange equations in (8), (9), (10),

$$H_\epsilon(z) = \frac{1}{2}\big(1 + \frac{2}{\pi} arctan\big(\frac{z}{\epsilon}\big)\big)$$

Accordingly, the regularized Dirac measure $\delta_\epsilon$ is defined as the derivative of $H_\epsilon$,

$$\delta_\epsilon(z) = \frac{\partial H_\epsilon}{\partial z} = \frac{1}{\pi} \frac{\epsilon}{\epsilon^2 + z^2}$$

To obtain discrete forms of the update equations (8), (9), (10) of $\Phi(x,y,t)$, $w_1(x,y,t)$, and $w_2(x,y,t)$, we use an implicit finite-difference scheme for discretizing the divergence operator, and then an iterative process until convergence to obtain desired segmentation and degradation model [12]. The principal steps of the algorithm are:

- Initialize $\Phi^0(x,y)$, $w_1^0(x,y)$, and $w_2^0(x,y)$ at $t = 0$.
- Compute intensity distribution parameters $\Lambda_1, \Lambda_2$ using (7).
- Solve (8), (9), and (10) in $\Phi^t(x,y)$, $w_1^t(x,y)$, and $w_2^t(x,y)$ to obtain $\Phi^{t+1}(x,y)$, $w_1^t(x,y)$ and $w_2^t(x,y)$.
- Check for convergence; otherwise, repeat for iteration $= t + 1$.

## III. EXPERIMENTAL VALIDATION

We tested the performance of the model on 6 brain MR volumes (2_4, 4_8, 5_8, 6_10, 15_3, and 16_3) obtained from the Internet Brain Segmentation Repository (IBSR) 20 normal subject dataset (Fig. 1). The 6 volumes are specifically selected as they have high noise and inhomogeneity artifacts, and are considered difficult cases for tissue segmentation in IBSR-20 dataset. We employ only real MR datasets in this study as simulated MR datasets often implicitly assume multiplicative image formation model in construction and, therefore, similar performance is expected as compared to methods that consider only the multiplicative intensity inhomogeneity component. The proposed method performed well and accurately estimated the multiplicative and additive components of the intensity inhomogeneities as shown in the $2^{nd}$ and $3^{rd}$ columns of Fig. 1. The $4^{th}$ and $5^{th}$ columns show the recovered image $\tilde{I}$ after estimating the degradation model and subsequent segmenting of the brain tissue, respectively.

To illustrate the significance of including the additive component $w_2$ along with the multiplicative component $w_1$, we compared tissue segmentation results from proposed method ($5^{th}$ column) with the results when using only the multiplicative component for intensity inhomogeneity correction ($6^{th}$ column). Table I shows a quantitative comparison using Jaccard Index (Tanimoto Index) as the evaluation metric for calculating overlap between the obtained segmentation and

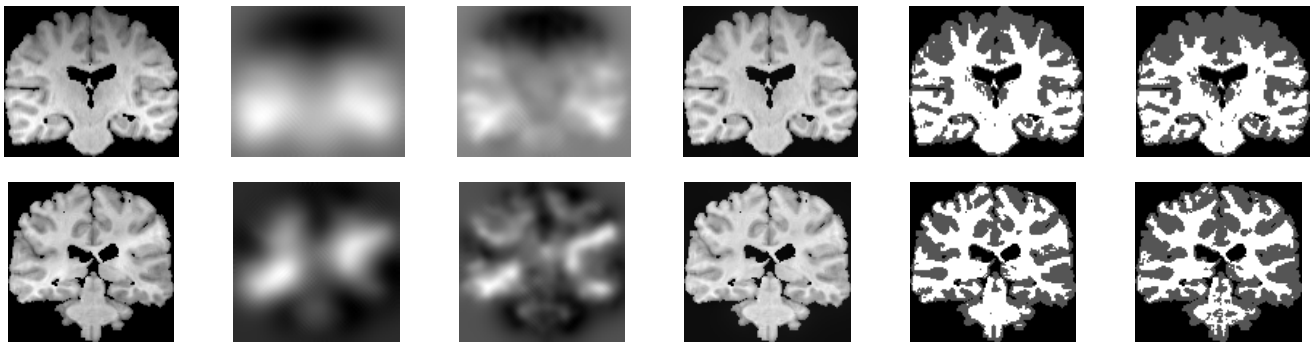

Fig. 1: Results of the proposed approach showing (a) the original images with intensity inhomogeneities ($1^{st}$ column), (b) the estimated multiplicative component ($2^{nd}$ column), (c) the estimated additive component ($3^{rd}$ column), (d) the recovered image $\tilde{I}$ ($4^{th}$ column), (e) tissue segmentation ($5^{th}$ column) using proposed model, and (f) tissue segmentation when only multiplicative component is considered ($6^{th}$ column) in the image degradation model.

TABLE I: Significance of Modeling Additive Intensity Inhomogeneity

| Method | $J^{WM}$ | $J^{GM}$ |
|---|---|---|
| Proposed Model | 0.6708±0.0309 | 0.7523±0.0191 |
| Only Multiplicative Model | 0.5463±0.0356 | 0.7063±0.0195 |
| No Inhomogeneity Correction | 0.2780±0.1938 | 0.3487±0.1564 |

the ground truth segmentation for white matter ($J^{WM}$) and gray matter ($J^{GM}$) tissue classes. We additionally compare proposed method with the segmentation results when no intensity inhomogeneity correction is performed to illustrate the relative gain in segmentation performance. The results suggest that including the additive component in the degradation model significantly improves the intensity inhomogeneity correction ($p < 0.01$ assessed using Wilcoxon rank sum test), thereby resulting in more accurate brain tissue segmentation. Visual comparisons between segmentation results in Fig. 1 show that the multiplicative component alone is insufficient to accurately model high intensity inhomogeneity regions ($6^{th}$ column) in MR images. The proposed method on the other hand ($5^{th}$ column), uses both additive and multiplicative components to more accurately account for the intensity inhomogeneities.

## IV. CONCLUSION

In this study, we have developed a variational level set approach for intensity inhomogeneity correction in brain MR images that combines the estimation of intensity inhomogeneities with tissue segmentation. Unlike the majority of the existing methods for intensity inhomogeneity correction, we develop a variation of a degradation model that includes both multiplicative and additive intensity inhomogeneity components. We illustrate the significance of the additive component by showing improved tissue segmentation relative to segmentation using only the multiplicative intensity inhomogeneity component. In the future, we plan to quantitatively evaluate the effectiveness of the proposed model for estimating intensity inhomogeneities in MR images.


## ACKNOWLEDGMENT

The 20 normal MR brain data sets and their manual segmentations were provided by the Center for Morphometric Analysis at Massachusetts General Hospital and are available at http://www.cma.mgh.harvard.edu/ibsr/.


## REFERENCES


[1] B. R. Condon, J. Patterson, D. Wyper, A. Jenkins, and D. M. Hadley, "Image non-uniformity in magnetic resonance imaging: its magnitude and methods for its correction," *British Journal of Radiology*, vol. 60, no. 709, pp. 83–87, 1987. [Online]. Available: http://bjr.birjournals.org/content/60/709/83.short

[2] A. Simmons, P. S. Tofts, G. J. Barker, and S. R. Arridge, "Sources of intensity nonuniformity in spin echo images at 1.5 t," *Magnetic Resonance in Medicine*, vol. 32, no. 1, pp. 121–128, 1994. [Online]. Available: http://dx.doi.org/10.1002/mrm.1910320117

[3] R. Stollberger and P. Wach, "Imaging of the active b1 field in vivo," *Magnetic Resonance in Medicine*, vol. 35, no. 2, pp. 246–251, 1996. [Online]. Available: http://dx.doi.org/10.1002/mrm.1910350217

[4] B. Johnston, M. Atkins, B. Mackiewich, and M. Anderson, "Segmentation of multiple sclerosis lesions in intensity corrected multispectral mri," *Medical Imaging, IEEE Transactions on*, vol. 15, no. 2, pp. 154 –169, apr 1996.

[5] M. Tincher, C. Meyer, R. Gupta, and D. Williams, "Polynomial modeling and reduction of rf body coil spatial inhomogeneity in mri," *Medical Imaging, IEEE Transactions on*, vol. 12, no. 2, pp. 361 –365, jun 1993.

[6] B. Dawant, A. Zijdenbos, and R. Margolin, "Correction of intensity variations in mr images for computer-aided tissue classification," *Medical Imaging, IEEE Transactions on*, vol. 12, no. 4, pp. 770 – 781, dec 1993.

[7] C. Meyer, P. Bland, and J. Pipe, "Retrospective correction of intensity inhomogeneities in mri," *Medical Imaging, IEEE Transactions on*, vol. 14, no. 1, pp. 36 –41, mar 1995.

[8] L. Wang, H.-M. Lai, G. J. Barker, D. H. Miller, and P. S. Tofts, "Correction for variations in mri scanner sensitivity in brain studies with histogram matching," *Magnetic Resonance in Medicine*, vol. 39, no. 2, pp. 322–327, 1998. [Online]. Available: http://dx.doi.org/10.1002/mrm.1910390222

[9] U. Vovk, F. Pernus, and B. Likar, "A review of methods for correction of intensity inhomogeneity in mri," *Medical Imaging, IEEE Transactions on*, vol. 26, no. 3, pp. 405 –421, march 2007.

[10] S. Osher and J. A. Sethian, "Fronts propagating with curvature dependent speed: Algorithms based on Hamilton-Jacobi formulations," *Journal of Computational Physics*, vol. 79, no. 1, pp. 12–49, 1988.

[11] L. Evans, "Partial differential equations," *Providence, R1:American Math. Soc.*, 1998.

[12] T. F. Chan and L. A. Vese, "Active contours without edges," 2001.